


Cite this: *RSC Adv.*, 2023, 13, 33446

Characterization of organic release kinetics in particleboard using a dual model fitting methodology†

Guodong Yuan, * Huiwen Yuan, Yingfeng Zhao and Zhi Liang

In modern society, people spend most of their time indoors engaging in their work and home life. However, indoor air pollution is a potential risk to health, and it is associated with many diseases. Wooden furniture, as the most popular indoor furniture used in modern times, is a major source of indoor air pollution, so it has become imperative to explore the composition and release kinetics characteristics of toxic and hazardous substances from wood-based panels. In this study, thermal desorption-gas chromatography-mass spectrometry (TD-GC-MS) was used to detect the release of organic compounds from wood panels, and determine the release kinetics of the organic compounds dimethyl acetal, phenol, toluene and decanoic acid via bi-exponential and mass transfer models to provide a theoretical basis for targeted pollution prevention and control. In this project, a climate chamber method was used to conduct a 120 h continuous sampling of the release concentration of compounds from wood panels. The TD-GC-MS method was used to analyze the sampling tubes, and the concentration–time data were fitted to the bi-exponential and mass transfer models. The emission factor equation was obtained from the bi-exponential model. The critical physical parameters, such as the initial internal release concentration C_0 , internal diffusion rate D_m , and solid-phase/gas-phase partition coefficient K , were obtained from the mass transfer model. Finally, it was found that dimethyl acetal and toluene were easily and rapidly released into the air, while phenol and decanoic acid were slowly released into the ambient air. The two sets of release kinetics characteristics provide an essential theoretical basis for targeted pollution prevention and control, as well as a methodological path for studying the release kinetics of different toxic and hazardous substances.

Received 29th May 2023
Accepted 29th October 2023

DOI: 10.1039/d3ra03587e

rsc.li/rsc-advances

1 Introduction

Air pollution has always been associated with chimneys and car exhaust in people's minds, as forms of outdoor air pollution. However, indoor air pollution (IAP) has not been given sufficient attention, which is more closely related to people's daily work and home life. 3.2 million people died of IAP-induced disease in the global world in 2020. IAP induces many types of conditions, such as asthma, stroke, heart disease, Alzheimer's disease, and even leukemia and lung cancer. People spend 80–90% of their life indoors in industrialized countries, such as in the house, in the office, at school, and in business workplaces. IAP thus has adverse effects on health and quality of life.^{1–3}

Through an in-depth analysis of the history of IAP, the corresponding prevention, risk exposure assessment research,

traceability, distribution, migration, degradation, intake, and absorption are necessary for exposure analysis and risk assessment. Further research, prevention and control should be carried out for the community with a shared interest in the future of humankind.^{4,5}

Indoor air quality impacts on the comfort, health, and happiness of human life, and poor quality air affects the respiratory and cardiovascular systems.^{6–10} Governments and international agencies have continuously set standard values for air quality. The German Environment Agency has set limits for 58 compounds, and China has also set limits on 13 compounds.¹¹ Moreover, the field of indoor air chemistry faces more great challenges arising from novel materials applications and population density growth.^{5,12–14}

IAP comprises formaldehyde, volatile organic compounds (VOCs), *etc.* Formaldehyde pollution draws significant attention, especially in newly decorated houses.^{15,16} However, VOCs, which represent more toxic and hazardous substances, have not received sufficient research attention.¹⁷

Wooden furniture is widely used in human life. However, wooden furniture releases large amounts of VOCs, which seriously impact human health as an essential pollution source in

National Center of Inspection & Testing on Building Materials Products Quality (Nanjing), Nanjing Institute of Product Quality Inspection (Nanjing Institute of Quality Development and Advanced Technology Application), Nanjing 211102, China. E-mail: DG1524109@smail.nju.edu.cn

† Electronic supplementary information (ESI) available. See DOI: <https://doi.org/10.1039/d3ra03587e>



indoor air.^{18–21} Artificial board is the main material of wooden furniture, wherein volatile substances are mainly contained in the wood itself and are introduced during materials processing, including through the use of adhesives and other such compounds. Therefore, it is meaningful to research the toxic and harmful substances and their release from wooden panels.^{22,23} Moreover, the irritating odor from wooden furniture affects the comfort of humans indoors, which is also a severe problem.²⁴ The analysis method widely used in wooden furniture testing is gas chromatography-mass spectrometry (GC-MS).^{13,20,22,25–27}

To accurately determine the principles governing the release of VOCs from wooden panels and wooden furniture, some physical parameters are essential, such as the internal initial release concentration, internal diffusion rate, and partition constants of organic compounds in the panels and air.^{23,28–32} There are two significant ways in which organic compounds in IAP affect the quality of life: one is the health hazards that arise from the pollution,³³ and the other is the odor impact of the pollutants.^{24,34}

Existing studies usually use an exponential model or mass-transfer model for individual study.³⁵ Exponential modeling can only reveal some of the apparent parameters of release kinetics, but cannot explain the intrinsic mechanisms of release kinetics, while the mass-transfer model can be used to understand the release concentration, the internal diffusion rate, the partition coefficient, the convective mass transfer coefficient and the mass-transfer Bivouac number, and other parameters, in terms of the release kinetics of a certain compound in a certain type of material sheet. The combination of the two methods is mutually beneficial, in corroborating and complementing each other, and this study combines the two methods to provide a more comprehensive and scientific explanation of the release kinetics of compounds from wood-based panels.

2 Materials and methods

2.1 Particleboard

The particleboard was made of wood chips and adhesive glued together by hot calendering. The particleboard in the experiment was purchased from the market, the panels were cut to 0.5 m × 0.5 m, and the thickness was 0.018 m. The edge of the panels was sealed with aluminum foil to ensure the organic compounds were released from the panel surface in the experiment. The panels were wrapped up before use and kept in a cool and dry place.

2.2 Climate chamber

The model of the climate chamber was Espec VOC-010, and the internal volume was 1 m³. The temperature (°C), the relative humidity (RH), and the air change rate (ACR) were controlled. The climate chamber was cleaned at 250 °C before new experiments were conducted. The experimental conditions were 23 °C, 50% RH, and an ACR of 1 m³ h^{−1}.

2.3 Sampling method

The air sampling equipment used for this method was a GL Sciences SP208Dual II instrument. One wooden panel was placed

on a metal stand in the Espec VOC emission test chamber, and the plane of the wooden board was parallel to the airflow direction. The air sampler and the Tenax-TA sampling tube collected the air sample from the climate chamber. The sampling rate was 1 L min^{−1}, and the sampling time was 10 min. The release area of the wooden panel was 0.5 m². The Espec chamber came with a clean air producing unit that removed unwanted gas in the air. The chamber was baked at high temperature for 24 h prior to the test, and after this time the temperature was reduced to the test temperature and equilibrium stabilized, and a blank background control was performed.

2.4 Analysis method

The method of VOC detection was thermal desorption-gas chromatography-mass spectrometry (TD-GC-MS, TD: TD100-xr, Markes International, GC: 7890A, MS: 5975C inert MSD with Triple-Axis Detector, Agilent Technologies). Qualitative analysis involved comparison with the NIST database. Quantitative analysis was calibrated to the standard curve of toluene. The climate chamber and adsorbent tube VOCs were subjected to a blank control test. This method is the current standard analytical method for studying the concentration of VOC compounds released, with instrumentation metered, compositional analysis confirmed using the NIST mass spectrometry database, and concentration quantified using an external standard curve based on toluene. The qualitative and quantitative ions (*m/z*) for each compound are shown in Table S2.†

2.5 Release kinetics model of the VOCs

2.5.1 Bi-exponential model. The bi-exponential model was adopted to describe the release process of the VOCs and determine the emission factor equation. The equation features two critical parameters: release rate and decay rate.

The equation is as follows:

$$E(t) = E_1(t) + E_2(t) = E_1(0)e^{-k_1t} + E_2(0)e^{-k_2t} \quad (1)$$

where $E(t)$ (mg m^{−2} h^{−1}) is the release rate of the VOCs; $E_1(t)$ and $E_2(t)$ (mg m^{−2} h^{−1}) are the release rate of the VOCs from phases 1 and 2, respectively; $E_1(0)$, $E_2(0)$ (mg m^{−2} h^{−1}) are the initial release rate of VOCs from phases 1 and 2, respectively; k_1 , k_2 (h^{−1}) are the release rate delay constants of VOCs from phases 1 and 2, respectively; and t (h) is the time. Phase 1 refers to the molecules that initially accumulate on the surface of the plate and are released into the chamber space, while phase 2 refers to the molecules that subsequently diffusely migrate from the interior of the plate to the surface of the plate and are released into the chamber space, with the two components being in different dynamically trending environments.

It was assumed that the amount of adsorbed VOCs on the climate chamber interior was negligible. The mass balance equation in the climate chamber is as follows:

$$VdC(t) = AE(t)dt - QC(t)dt \quad (2)$$

where V (m³) is the interior space volume of the climate chamber; A (m²) is the release surface area; Q (m³ h^{−1}) is the



flow rate of the climate chamber; and C (mg m^{-3}) is the concentration of VOCs in the climate chamber.

Assuming the initial concentration of VOCs to be zero, the following equation can be derived from the two equations above:

$$C(t) = LE_1(0)(e^{-k_1 t} - e^{-Nt})/(N - k_1) + LE_2(0)(e^{-k_2 t} - e^{-Nt})/(N - k_2) \quad (3)$$

where L is loading rate ($\text{m}^2 \text{m}^{-3}$) and N is the air exchange rate (h^{-1}).

The emission factor of the panel is:

$$E(t) = E_1 e^{-k_1 t} + E_2 e^{-k_2 t} \quad (4)$$

2.5.2 Mass transfer model. The mass transfer model was adopted to describe the vital physical parameters C_0 , D_m and K . Two stages are involved in VOC release from wooden panels: compound migration from the interior to the surface of the panels and compound release from the panel surface to the surrounding air. The internal initial release concentration C_0 represents the initial content of compounds in the panels, which is the basis of release. The internal diffusion rate D_m is the internal migration rate of compounds from the interior of the panels to the surface. The gas–solid partition coefficient K is the distribution ratio between the surrounding air and the panel surface, representing a tendency for release of compounds from the panel surface to the air (Fig. 1).

The equations are as follows:

$$C_a(t) = C_{in} + \left[2C_0\beta \sum_{n=1}^{\infty} \frac{q_n \sin q_n}{G_n} + 2\alpha C_{in} \sum_{n=1}^{\infty} \frac{K\text{Bi}_m^{-1} q_n \sin q_n - \cos q_n}{G_n} + 2C_{a,0} \sum_{n=1}^{\infty} \frac{q_n^2 (\cos q_n - K\text{Bi}_m^{-1} q_n \sin q_n)}{G_n} \right] e^{-D_m \delta^{-2} q_n^2 t} \quad (5)$$

$$\text{Bi}_m = h_m \delta / D_m, \alpha = Q \delta^2 / V D_m, \beta = A \delta / V \quad (6)$$

$$G_n = [K\beta + (\alpha - q_n^2) K\text{Bi}_m^{-1} + 2] q_n^2 \cos q_n + [K\beta + (\alpha - 3q_n^2) K\text{Bi}_m^{-1} + \alpha - q_n^2] q_n \sin q_n \quad (7)$$

The mass transfer Biovolt number, Bi_m , is the ratio of diffusive mass transfer resistance inside the material to convective mass transfer resistance outside the material. α is the air exchange rate; β is the ratio of the materials volume to the climate chamber volume; A is the surface area of the panel (m^2); δ is half of the panel thickness value (m); V is the interior volume of the climate chamber (m^3); Q is the air flow rate in the climate chamber ($\text{m}^3 \text{h}^{-1}$); K is the distribution factor between the panel surface and the surrounding air; and h_m is the convective mass transfer coefficient (m s^{-1}).

q_n is the positive root of the following equations:

$$q_n \tan q_n = \frac{\alpha - q_n^2}{K\beta + (\alpha - q_n^2) K\text{Bi}_m^{-1}}, (n = 1, 2, \dots) \quad (8)$$

The real-time release concentration conforms to the following equation:

$$C_a(t) - C_{in} = \left[2C_0\beta \frac{q_1 \sin q_1}{G_1} + 2\alpha C_{in} \frac{K\text{Bi}_m^{-1} q_1 \sin q_1 - \cos q_1}{G_1} + 2C_{a,0} \frac{q_1^2 (\cos q_1 - K\text{Bi}_m^{-1} q_1 \sin q_1)}{G_1} \right] e^{-D_m \delta^{-2} q_1^2 t} \quad (9)$$

q_1 is the first positive root of the equation. G_1 is the first root of the equation. The equation can be further transformed into the following equation:

$$\ln(C_a(t) - C_{in}) = -D_m \delta^{-2} q_1^2 t + \ln \left[2C_0\beta \frac{q_1 \sin q_1}{G_1} + 2\alpha C_{in} \frac{K\text{Bi}_m^{-1} q_1 \sin q_1 - \cos q_1}{G_1} + 2C_{a,0} \frac{q_1^2 (\cos q_1 - K\text{Bi}_m^{-1} q_1 \sin q_1)}{G_1} \right] \quad (10)$$

The linearization of the equation is as follows:

$$\ln(C_a(t) - C_{in}) = kt + b \quad (11)$$

where k is the slope and b is the intercept distance.

$$k = -D_m \delta^{-2} q_1^2 \quad (12)$$

$$b = \ln \left[2C_0\beta \frac{q_1 \sin q_1}{G_1} + 2\alpha C_{in} \frac{K\text{Bi}_m^{-1} q_1 \sin q_1 - \cos q_1}{G_1} + 2C_{a,0} \frac{q_1^2 (\cos q_1 - K\text{Bi}_m^{-1} q_1 \sin q_1)}{G_1} \right] \quad (13)$$

To obtain a solution to the equation, the parameters D_m , h_m and K should be estimated using PARAMS. Igor Pro and Wolfram were used to process the data, and simulation validation was executed using the IAQX of the Environmental Protection Agency (EPA). The basic condition for both models was the assumption that the air was well mixed. Eqn (5) is derived from Fick's second law of internal diffusion processes, boundary conditions for boundary convection processes, and the conservation of mass and transform of Laplace. To solve eqn (5), you need to solve eqn (7) and (8) firstly. Specific solutions can be found in the literature.³⁶

3 Results and discussion

3.1 Summary of important detected substance in particleboard

A particleboard was chosen as a typical sample for the research on the release kinetics. The particleboard was cut to $0.5 \text{ m} \times 0.5 \text{ m}$ and placed in the middle of a cleaned climate chamber, and the plane of the board was parallel to the direction of the fan's airflow in the climate chamber. The experiment conditions were 23°C , 50% RH, high fan strength, and an ACR of 1 h^{-1} . The determination conditions of TD-GC-MS are displayed in Table



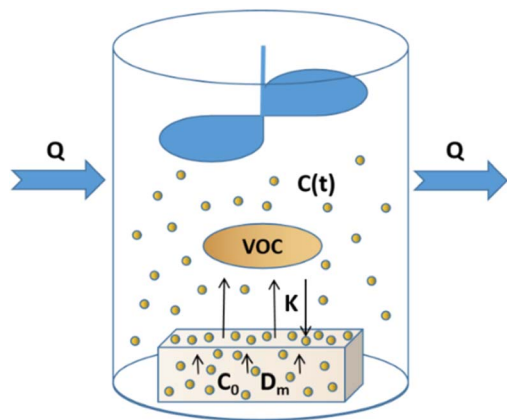


Fig. 1 Schematic diagram of the panel VOC release test.

S1.† The total tracking sampling time was 120 h. Significant detections are shown in Table S2.†

Dimethyl acetal, toluene, phenol and decanoic acid were chosen as representative research compounds based on their retention time, odor, and toxicity. Toluene is one of the most concerning toxic and hazardous substances and the semi-quantitative reference for this experimental method. Dimethyl acetal has a low boiling point and an irritating odor. Phenol has a medium boiling point, particular odor, and high toxicity. Decanoic acid has a higher boiling point and an unpleasant odor. It was essential to compare the differences in the release pattern of the four compounds.

3.2 Bi-exponential model fitting

The entire release involves a molecular diffusion process from the interior to the panel's surface and a molecular migration process from the panel's surface to the surrounding air in the climate chamber. These two processes are concurrent and simultaneous.

Table 1 Bi-exponential model fitting

| Compound name | Emission factor equations of the panels |
|-----------------|---|
| Dimethyl acetal | $E(t) = 0.0677 \times e^{-1.16t} + 0.0114 \times e^{-0.01t}$ |
| Phenol | $E(t) = 0.0045 \times e^{-0.0048t} + 0.003 \times e^{-0.13t}$ |
| Toluene | $E(t) = 0.11 \times e^{-1.9t} + 0.012 \times e^{-0.003t}$ |
| Decanoic acid | $E(t) = 0.022 \times e^{-0.26t} + 0.001 \times e^{-0.005t}$ |

In the first process, the release rate is mainly dominated by the migration rate of molecules from the panel surface to the surrounding air. Furthermore, in the second process, the release rate is dominated by the diffusion process of molecules from the interior to the surface. A bi-exponential model was used to describe the entire process.

As shown in Fig. 2 and Table 1, four compounds were selected: dimethyl acetal, phenol, toluene, and decanoic acid. Release curves were plotted based on the release concentrations of these compounds at different time points. Data analysis proved that the IAQX software fitting was also performed based on these formula sets because of the same results obtained. The initial rapid release came from compounds that had been enriched on the surface of the panels before being placed in the climate chamber. Moreover, fast dissipation arose from the air exchange. The trend then slowed as the release rate-limiting step shifted to internal diffusion.

The initial release of dimethyl acetal and toluene was faster than phenol and decanoic acid on comparing the release curves of the four compounds. This means that dimethyl acetal and toluene are more easily released from the panel surface to the climate chamber air than phenol and decanoic acid. The biexponential model fitting parameters are shown in Tables S3, S5, S7 and S9.†

3.3 Mass transfer model fitting

The mass transfer model has three critical parameters: C_0 , D_m and K . C_0 is the initial release concentration, where a high value

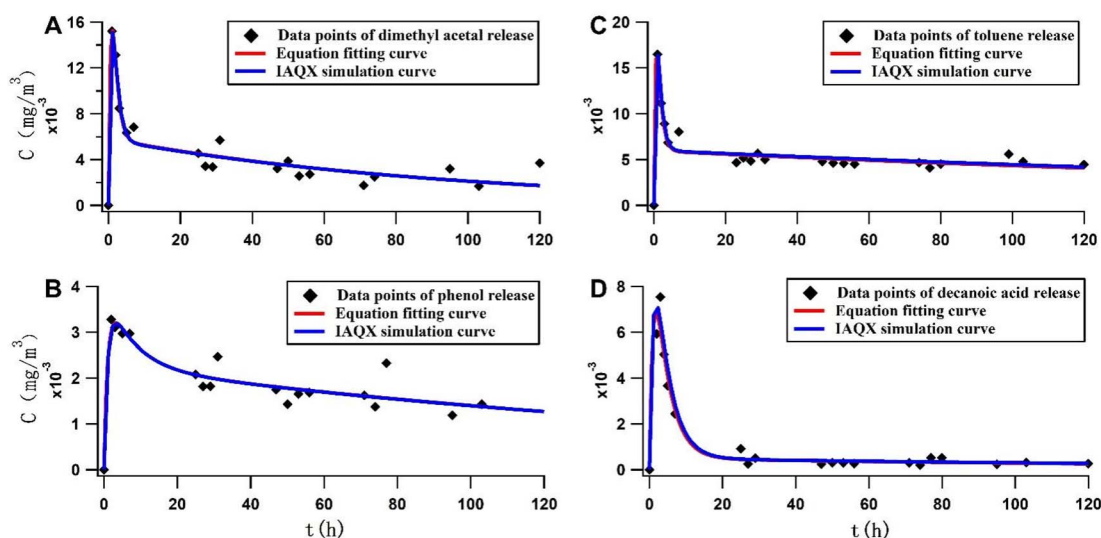


Fig. 2 Bi-exponential model fitting of the four compounds released over the entire process: (A) dimethyl acetal, (B) phenol, (C) toluene, and (D) decanoic acid. The curves fitted using the formula overlap with the IAQX software fitting results.



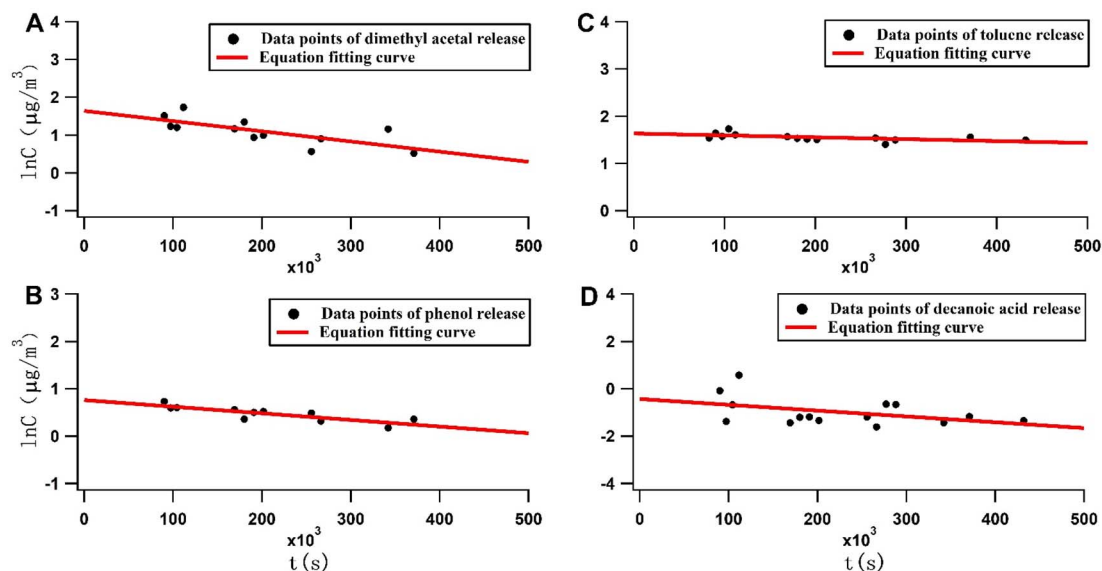


Fig. 3 Mass transfer model fitting of the release of four compounds: (A) dimethyl acetal, (B) phenol, (C) toluene, and (D) decanoic acid.

indicates a high content of compounds in the material. D_m is the internal diffusion rate, where a high value indicates fast compound migration from the interior to the panel's surface. K is the distribution factor, where a high value means that the compound shows preferential solid-phase adsorption at equilibrium between the solid and air phases (Fig. 3 and Table 2).

Several physical parameters assist in characterizing the release kinetics. When Bi_m/K is >35 , the compound release is limited by the migration rate from the interior to the surface. When Bi_m/K is <1 , the compound release is limited by the migration rate from the surface to the surrounding air. When Bi_m/K is between 1 and 35, the compound release characteristics require further experimental determination.

The four compounds exhibit different release kinetics properties by comparing the physical parameters obtained by

fitting them using a mass transfer model (Table 3). Dimethyl acetal was most easily released into the air as a result of its lower K value and the higher h_m value. Toluene was also quickly released into the air due to its lower K value. Phenol tends to collect on the panel's surface and is released into the air more slowly due to high D_m and K values. Decanoic acid also tends to collect on the panel's surface and is released into the air the slowest due to its high D_m and K values and low h_m value. In terms of Bi_m/K , the values of decanoic acid and phenol are <1 , and the values of toluene and dimethyl acetal are between 1 and 35. This means that the release rate-limiting step of decanoic acid and phenol is the migration rate from the surface to the air. In contrast, the toluene and dimethyl acetal release rate-limiting step is the diffusion rate from the interior to the surface. It was found that the internal diffusion rate of the

Table 2 Mass transfer model fitting

| Compound name | Mass transfer model fitting equation |
|-----------------|---|
| Toluene | $\ln(C_a(t) - C_{in}) = -24683.9 \times D_m \times t + \ln(3.06 \times 10^{-6} \times C_0)$ |
| Dimethyl acetal | $\ln(C_a(t) - C_{in}) = -6870.6 \times D_m \times t + \ln(7.4 \times 10^{-5} \times C_0)$ |
| Decanoic acid | $\ln(C_a(t) - C_{in}) = -1089.0 \times D_m \times t + \ln(1.3 \times 10^{-9} \times C_0)$ |
| Phenol | $\ln(C_a(t) - C_{in}) = -3520.4 \times D_m \times t + \ln(2.95 \times 10^{-7} \times C_0)$ |

Table 3 Key parameters of release kinetics

| Key parameters | Dimethyl acetal | Toluene | Phenol | Decanoic acid |
|--|-----------------------|-----------------------|------------------------|-----------------------|
| C_0 ($\mu\text{g m}^{-3}$) | 4.3×10^3 | 1.7×10^6 | 7.3×10^6 | 5.0×10^8 |
| D_m ($\text{m}^2 \text{s}^{-1}$) | 3.9×10^{-10} | 1.6×10^{-11} | 3.98×10^{-10} | 2.3×10^{-9} |
| K^a | 73.98 | 706 | 2.47×10^4 | 5.047×10^6 |
| h_m (m s^{-1}) ^a | 5.06×10^{-4} | 4.24×10^{-4} | 4.39×10^{-4} | 3.52×10^{-4} |
| Bi_m/K^a | 2.4 | 15.94 | 0.565 | 0.15 |

^a The data was estimated by PARAMS.



larger molecular weight decanoic acid was surprisingly faster compared to the smaller molecular weight dimethyl acetal. We believe that we can refer to the molecular sieve column principle, in that the diffusion transport of compounds with larger molecules in a sieve pore-shaped material adopts the shortest path, so compounds with larger molecular weights will have a faster rate of internal diffusion. The mass transfer model fitting parameters are shown in Tables S4, S6, S8 and S10.†

4 Conclusions

In this study, the gas released from wood panels in a climate chamber was sampled and analyzed using TD-GC-MS. Bi-exponential and mass transfer models were found to fit the data.

This study combined bi-exponential and mass transfer models to determine the release kinetics of the compounds in panels. The release rate-limiting steps were determined by differentiating the C_0 , D_m , K , and Bi_m/K values of the four representative compounds to obtain two groups of release kinetics characteristics.

The release kinetics characteristics of toluene were medium concentration and quick release due to a lower K and higher C_0 ; the release kinetics characteristics of dimethyl acetal were low concentration and immediate release due to a lower K and higher h_m ; the release kinetics characteristics of phenol were surface enrichment and medium release due to a medium D_m , medium h_m and higher K ; and the release kinetics characteristics of decanoic acid were low concentration, easy surface enrichment and slow release due to higher D_m , higher K and lower h_m .

This indicates that toluene and dimethyl acetal are more inclined to be released into the air, and window ventilation has a higher emission efficiency, making them more suitable for adsorption degradation-type governance programs, such as maximizing window ventilation, air purifier adsorption, activated carbon adsorption, *etc.* However, decanoic acid and phenol are more inclined to be enriched on the surface of a panel, so production source control becomes more critical, making them more suitable for surface spraying degradation-type governance programs, such as photocatalysts, *etc.*

Through the study of the release kinetics characteristics of organic compounds, the pollution characteristics of indoor furniture products and decoration and building materials products can be more accurately assessed, which is conducive to optimizing the selection of pollutant control means and more accurately calculating the carbon emission characteristics of pollutants, promoting the scientific improvement of indoor environmental evaluation and environmental management, as well as the formulation of more scientifically effective targeted treatment programs.

In the future, based on the release kinetics research, the project will continue to focus on expanding research categories, exploring new pollutants, prevention and control research and information technology-assisted research.

The study of the release kinetics of compounds in wood-based panels can provide a theoretical basis and

methodological reference for the tracing of IAP sources, multi-parameter dynamic identification of IAPs, high-efficiency low-carbon purification and online monitoring.

Author contributions

Guodong Yuan: investigation, experiment, data analysis, writing; Huiwen Yuan: discussion, supervision, assistance, review, proposal; Yingfeng Zhao: supervision, review, proposal; Zhi Liang: consulting, proposal.

Conflicts of interest

There are no conflicts of interest to declare.

Acknowledgements

This work was supported by the Science and Technology Projects of Jiangsu Provincial Administration for Market Regulation [KJ2023033] and the Science and Technology Projects of Nanjing Administration for Market Regulation [KJ2021020].

References

- 1 C. J. Weschler, *Indoor Air*, 2011, **21**, 205–218.
- 2 P. Wolkoff, *Int. J. Hyg. Environ. Health*, 2018, **221**, 376–390.
- 3 W. Ye, X. Zhang, J. Gao, G. Cao, X. Zhou and X. Su, *Sci. Total Environ.*, 2017, **586**, 696–729.
- 4 T. Salthammer, Y. Zhang, J. Mo, H. M. Koch and C. J. Weschler, *Angew. Chem., Int. Ed.*, 2018, **57**, 12228–12263.
- 5 E. Uhde and T. Salthammer, *Atmos. Environ.*, 2007, **41**, 3111–3128.
- 6 K. W. Tham, *Energy Build.*, 2016, **130**, 637–650.
- 7 A. Cincinelli and T. Martellini, *Int. J. Environ. Res. Public Health*, 2017, **14**, 1286.
- 8 R. Menghi, S. Ceccacci, A. Papetti, M. Marconi and M. Germani, *Procedia Manuf.*, 2018, **21**, 486–493.
- 9 E. Braunwald, *Eur. Heart J.*, 2023, **44**, 1679–1681.
- 10 J. A. Hoskins, *Indoor Built Environ.*, 2003, **12**, 427–433.
- 11 G. Settimo, Y. Yu, M. Gola, M. Buffoli and S. Capolongo, *Atmosphere*, 2023, **14**, 633.
- 12 D. K. Farmer, *Anal. Chem.*, 2019, **91**, 3761–3767.
- 13 D. K. Farmer, M. E. Vance, J. P. D. Abbatt, A. Abeleira, M. R. Alves, C. Arata, E. Boedicker, S. Bourne, F. Cardoso-Saldaña, R. Corsi, P. F. DeCarlo, A. H. Goldstein, V. H. Grassian, L. Hildebrandt Ruiz, J. L. Jimenez, T. F. Kahan, E. F. Katz, J. M. Mattila, W. W. Nazaroff, A. Novoselac, R. E. O'Brien, V. W. Or, S. Patel, S. Sankhyan, P. S. Stevens, Y. Tian, M. Wade, C. Wang, S. Zhou and Y. Zhou, *Environ. Sci.: Processes Impacts*, 2019, **21**, 1280–1300.
- 14 J. M. Mattila, C. Arata, A. Abeleira, Y. Zhou, C. Wang, E. F. Katz, A. H. Goldstein, J. P. D. Abbatt, P. F. DeCarlo, M. E. Vance and D. K. Farmer, *Environ. Sci. Technol.*, 2022, **56**, 109–118.
- 15 S. B. Holøs, A. Yang, M. Lind, K. Thunshelle, P. Schild and M. Mysen, *Int. J. Vent.*, 2019, **18**, 153–166.

- 16 X. Liu, M. A. Mason, Z. Guo, K. A. Krebs and N. F. Roache, *Atmos. Environ.*, 2015, **122**, 561–568.
- 17 B. Zabiegała, *Pol. J. Environ. Stud.*, 2006, **15**, 383–393.
- 18 P. Harb, N. Locoge and F. Thevenet, *Chem. Eng. J.*, 2018, **354**, 641–652.
- 19 C. Jiang, S. Li, P. Zhang and J. Wang, *Build. Environ.*, 2013, **69**, 227–232.
- 20 S. Kim, Y.-K. Choi, K.-W. Park and J. T. Kim, *Bioresour. Technol.*, 2010, **101**, 6562–6568.
- 21 P. Wolkoff and G. D. Nielsen, *Atmos. Environ.*, 2001, **35**, 4407–4417.
- 22 S. Kim, J.-A. Kim, H.-J. Kim and S. Do Kim, *Polym. Test.*, 2006, **25**, 605–614.
- 23 J. Xiong, F. Chen, L. Sun, X. Yu, J. Zhao, Y. Hu and Y. Wang, *Build. Environ.*, 2019, **161**, 106237.
- 24 E. Gallego, X. Roca, J. F. Perales and X. Guardino, *J. Environ. Sci.*, 2009, **21**, 333–339.
- 25 S. K. Pang, H. Cho, J. Y. Sohn and K. D. Song, *Indoor Built Environ.*, 2007, **16**, 444–455.
- 26 X. Zhou, Z. Yan, X. Zhou, C. Wang, H. Liu and H. Zhou, *Chemosphere*, 2022, **308**, 136460.
- 27 K. A. Gorder and E. M. Dettenmaier, *Groundwater Monit. Rem.*, 2011, **31**, 113–119.
- 28 H. Wang, J. Zheng, T. Yang, Z. He, P. Zhang, X. Liu, M. Zhang, L. Sun, X. Yu, J. Zhao, X. Liu, B. Xu, L. Tong and J. Xiong, *Environ. Int.*, 2020, **142**, 105817.
- 29 Y. Wang, H. Wang, Y. Tan, J. Liu, K. Wang, W. Ji, L. Sun, X. Yu, J. Zhao, B. Xu and J. Xiong, *Atmos. Environ.*, 2021, **259**, 118510.
- 30 B. Xu, Y. Wang, D. Guo, Y. Gao, W. Liu, W. Wu, L. Sun, X. Yu, J. Zhao and J. Xiong, *Sci. Total Environ.*, 2022, **819**, 153126.
- 31 R. Zhang, H. Wang, Y. Tan, M. Zhang, X. Zhang, K. Wang, W. Ji, L. Sun, X. Yu, J. Zhao, B. Xu and J. Xiong, *Build. Environ.*, 2021, **196**, 107786.
- 32 X. Zhang, H. Wang, B. Xu, H. Wang, Y. Wang, T. Yang, Y. Tan, J. Xiong and X. Liu, *Environ. Int.*, 2022, **160**, 107064.
- 33 R. Tong, L. Zhang, X. Yang, J. Liu, P. Zhou and J. Li, *J. Cleaner Prod.*, 2019, **208**, 1096–1108.
- 34 C. Conti, M. Guarino and J. Bacenetti, *Environ. Int.*, 2020, **134**, 105261.
- 35 H. Shao, Y. Ren, Y. Zhang, C. Wu, W. Li and J. Liu, *RSC Adv.*, 2021, **11**, 26151–26159.
- 36 B. Deng and C. N. Kim, *Atmos. Environ.*, 2004, **38**, 1173–1180.

